An evaluation of the consistency of data and models for performance assessment: Divalent metal sorption on montmorillonite

Esra Orucoglu, Sylvain Grangeon, Jean-Charles Robinet, Benoît Madé, Christophe Tournassat

Applied Clay Science 261 (2024) 107569

Contents lists available at ScienceDirect

Applied Clay Science

journal homepage: www.elsevier.com/locate/clay

Research Paper

An evaluation of the consistency of data and models for performance assessment: Divalent metal sorption on montmorillonite

Esra Orucoglu [a,b,*], Sylvain Grangeon [a], Jean-Charles Robinet [d], Benoît Madé [d], Christophe Tournassat [b,c]

[a] BRGM, F-45060 Orléans, France
[b] ISTO, UMR 7327, Université d'Orléans, CNRS, BRGM, OSUC, Orléans, France
[c] Earth and Environmental Sciences Area, Lawrence Berkeley National Laboratory, Berkeley, CA, USA
[d] Andra, DISTEC/DRG Department, 1 – 7 rue Jean Monnet, 92298 Châtenay-Malabry, France

ARTICLE INFO

Keywords:
SCM
Minimalist model
Sorption
Divalent metal
Montmorillonite

ABSTRACT

A detailed analysis of literature data on the retention of divalent metal by purified montmorillonite or montmorillonite-rich material (e.g. bentonite) was conducted. Data for which sufficient experimental conditions were available were modeled with the 2SPNE SC/CE model available in the literature, and with a "minimalist" model, which uses a minimum number of parameters to reproduce the data.

A successful data modeling could only be achieved if considering (i) cation exchange competition with aqueous Ca^{2+} and Mg^{2+}, originating from the dissolution of the clay mineral itself or accessory minerals and (ii) precipitation, at high pH, of phases incorporating the divalent metal of interest. However, in many studies, the concentration of aqueous Ca^{2+} and Mg^{2+} and, more generally, a full characterization of solution composition (e.g., Si, Al, dissolved organic carbon, alkalinity) is not provided, thus impeding accurate data modeling. Further difficulties stem from uncertainties related to the nature of the solids precipitating at high pH and missing or inaccurate thermodynamic data related to mineral solubility.

Log K_D values cannot be predicted from available literature data with an accuracy better than ±1 log unit, without sorption data obtained on a material representative of in situ conditions. In addition, the most reactive sites, commonly referred to as strong sites, which have been characterized only on some, but not all, reference clay materials, should not be considered in blind predictions based on the mineralogical composition of clay materials.

1. Introduction

Engineered bentonite and natural clay rocks are commonly considered suitable barriers in geological (radioactive) waste repositories (Hautevelle et al., 2007; Lázár and Máthé, 2012; Grambow, 2016). Clay barriers limit radionuclide mobility in the geosphere and, hence, migration to the biosphere. First, their low permeability makes diffusion the main mechanism for aqueous species transport. Second, their adsorption capabilities associated with their high reactive surface area are efficient contributors to transport retardation for a large range of radionuclides. Third, clay minerals and their associated accessory minerals often provide near-neutral or alkaline as well as reductive conditions, which are favorable to the precipitation of radionuclides (Dähn et al., 2002; De Windt et al., 2004; Malekifarsani and Skachek, 2009; Altmann et al., 2012; Bardelli et al., 2014; Tournassat et al., 2015; Gailhanou et al., 2017).

The sorption (absorption, adsorption, precipitation including epitaxial growth, substitution, and incorporation) of radionuclides on clay materials is highly dependent on the nature of the clay minerals and on environmental physical and chemical properties such as pH, ionic strength, temperature, redox, and the overall chemical composition of the pore water, including major, minor and trace elements, which influence aqueous and surface speciation of radionuclides (Schlegel et al., 2001a, 2001b; Dähn et al., 2002, 2003; Lee et al., 2004; Tournassat et al., 2013; Orucoglu et al., 2018; Fan et al., 2019; Marques Fernandes and Baeyens, 2019). In performance assessment (PA) and safety assessment (SA) studies, sorption properties of clay barriers are most often predicted using the combination of a solubility limit in

* Corresponding author at: BRGM, F-45060 Orléans, France.
E-mail address: e.orucoglu@brgm.fr (E. Orucoglu).

https://doi.org/10.1016/j.clay.2024.107569
Received 12 February 2024; Received in revised form 4 September 2024; Accepted 5 September 2024
Available online 11 September 2024

combination with a K_D adsorption model, which relates the sorbed concentrations of radionuclides surface (C_{ads} in mol•kg$^{-1}_{solid}$) to their aqueous concentration at equilibrium (C_{eq} in mol•L$^{-1}_{solution}$) with a linear relationship: $K_D = C_{ads}/C_{eq}$. This very simple approach may be justified in modeling scenarios in which (1) the physicochemical conditions are considered to be constant, and (2) the concentrations of the radionuclides of interest are very low. If so, this approach still necessitates a selection of K_D values from data obtained with experimental conditions that are fully representative of in situ conditions. Mimicking the in situ conditions of clay rock porewater in laboratory experiments is notoriously difficult, especially in maintaining redox and carbonate system equilibrium conditions, and controlling trace elements concentrations (Claret et al., 2010; Beaucaire et al., 2012; Montavon et al., 2014; Grangeon et al., 2015; Gailhanou et al., 2017). Besides, in situ physicochemical conditions are only known within a range of uncertainty (Sochala et al., 2022). For these reasons, best estimates of K_D values are often sought by calibrating surface speciation models with experimental data that cover an extended range of environmental conditions representative of the storage environment (Bradbury and Baeyens, 1997; Bradbury et al., 2005; Marques Fernandes and Baeyens, 2019). These models can be further used to make predictions combined with sensitivity analysis and propagation of uncertainties for a large range of radionuclides and toxic chemicals representative of radioactive waste composition (Sochala et al., 2024).

For more than three decades, radioactive waste management agencies, such as Andra or NAGRA, have funded sorption experiments for clay minerals and clayey rocks. These data have been interpreted and quantified within the framework of surface complexation and cation exchange models (SCM and CE models, respectively) (Baeyens and Bradbury, 1997; Dähn et al., 2002; Tertre et al., 2005; Grambow et al., 2006; Bradbury and Baeyens, 2011; Pfingsten et al., 2011; Chen et al., 2014a; Orucoglu et al., 2018; Fralova et al., 2021), and linear free energy relationships (LFERs) have been made available to estimate the adsorption properties of contaminants for which experimental data are still missing (Bradbury and Baeyens, 2005a, 2009a). This knowledge obtained on reference clay minerals, such as Illite du Puy and montmorillonite samples from the Source Clay Repository, has been increasingly used to build models that predict the overall sorption properties of clayey rocks, using model additivity rules constrained with the mineral compositions of these rocks (Bradbury and Baeyens, 2000, 2011; Chen et al., 2014b; Marques Fernandes et al., 2015; Montavon et al., 2020).

However, surface complexation models lack an accepted uniform thermodynamic concept, and so, their parameters depend on the arbitrary choices of modelers (Kulik, 2009). In that sense, the modeling of adsorption data is never unique, and various models, using different molecular hypotheses and up-scaling simplifications, can lead to equally good fits of the reference data, while predicting different results in other scenarios (Tournassat et al., 2013).

The choice of the data set that is used to adjust model parameters is another source of the variability of adsorption model predictions. A surface speciation model calibrated for a specific clay mineral such as montmorillonite must not be used to predict the adsorption properties of another clay mineral such as illite, because of their differences in structural properties, particle size, and shape, which control the adsorption processes. Less obviously, a model calibrated with data obtained on a montmorillonite sample, e.g. the clay fraction of SWy-1 smectite, may be erroneous in predicting the data obtained on another montmorillonite sample, e.g. the clay fraction of MX80 bentonite, with deviations up to one order of magnitude (Grambow et al., 2006; Tournassat et al., 2013; Orucoglu et al., 2018). While some reasonable explanations can be put forward to explain the discrepancies, such as differences in layer composition, particle size, sample preparation, and experimental procedure, the absence of adsorption data consistency points out the possible problem of a lack of genericity for existing clay mineral surface speciation models. In turn, this possible lack of genericity questions the strategy of predicting the adsorption of clayey rock based on their mineralogical composition coupled with an additive adsorption model.

In this respect, the objective of the present study is quantifying errors made by reference models in the prediction of adsorption data, thereby enabling an objective estimation of the uncertainty of the predictions made by predictive additive models used for clayey rocks. To do so, it is necessary to decipher the discrepancies of model vs. data that can be properly reduced by considering differences in experimental procedures, from those that cannot be reduced without changing the surface speciation model parameters. In doing so, it was intended to isolate a minimum number of generic model parameters together with an estimation of the associated uncertainty for its use in an additive adsorption model. This work is focused on the adsorption of divalent metallic cations (Cd^{2+}, Co^{2+}, Cu^{2+}, Mn^{2+}, Ni^{2+}, Pb^{2+}) on montmorillonite surfaces.

2. Theoretical background and modeling strategies

2.1. Basic mechanisms

Wet chemistry experiments and spectrometric and diffractometric characterizations evidenced three main mechanisms responsible for the total uptake of divalent metals by clay minerals: cation exchange on basal surfaces, complexation on edge surfaces, and (surface) precipitation (Liu et al., 2022). Because of the complex chemistry and morphology of clay minerals, each of these processes occurs on a variety of sites at the clay mineral surfaces (Dähn et al., 2002, 2011; Churakov and Dähn, 2012). The relative importance of these processes depends mostly on pH, ionic strength, and aqueous concentration of the sorbed metal concentration (Fig. 1), as well as dissolved inorganic carbon concentration and the presence of competing cations (Charlet et al., 1993; Tournassat et al., 2013; Orucoglu et al., 2018). In short, cation exchange is favored by low ionic strengths because of a lesser competition with background electrolyte cations, while surface complexation is favored by a pH increase, which makes H^+ less competitive for edge surface complexation sites, and (surface) precipitation is favored by high pH values, high carbonate or bicarbonate concentration, and/or high concentration of the divalent metal of interest because it favors the supersaturation of the precipitating phases.

2.2. Reference models

Numerous surface complexation models coupled to cation exchange models have been proposed in the literature to describe adsorption data on clay mineral surfaces (Fletcher and Sposito, 1989; Turner et al., 1998; Barbier et al., 2000; Bradbury and Baeyens, 2002; Ikhsan et al., 2005; Tertre et al., 2005; Gu et al., 2010; Akafia et al., 2011; Ghayaza et al., 2011), but very few of them have been confronted successfully to a large range of experimental data (Tournassat et al., 2013). The two sites protolysis non-electrostatic surface complexation and cation exchange (2SPNE SC/CE) model, initially developed by Bradbury and Baeyens (1997, 1999, 2002), is a notable exception. This model has been effectively used to describe the adsorption of metallic cations, actinides, and lanthanides on montmorillonite and illite surfaces, at pH ranging from ~3 to ~10, at ionic strength ranging from 0.01 to 0.5, and with sorbate equilibrium concentrations ranging from 10^{-10} mol•L^{-1} to 10^{-2} mol•L^{-1} (Bradbury and Baeyens, 1997, 2009a, 2009b; Bradbury et al., 2005; Dähn et al., 2011; Marques Fernandes and Baeyens, 2019). In this model, the total adsorption is calculated with the combination of a cation exchange model, which describes the equilibrium of the solution composition with the planar surfaces exhibiting permanent structural charges, and a non-electrostatic surface complexation model for the adsorption processes taking place on the edge surfaces, which are mostly dependent on pH. The edge surfaces are described using two types of complexation sites: the so-called strong (≡S_SOH) and weak (≡S_WOH) sites, with, respectively, lower capacity/higher affinity, and higher

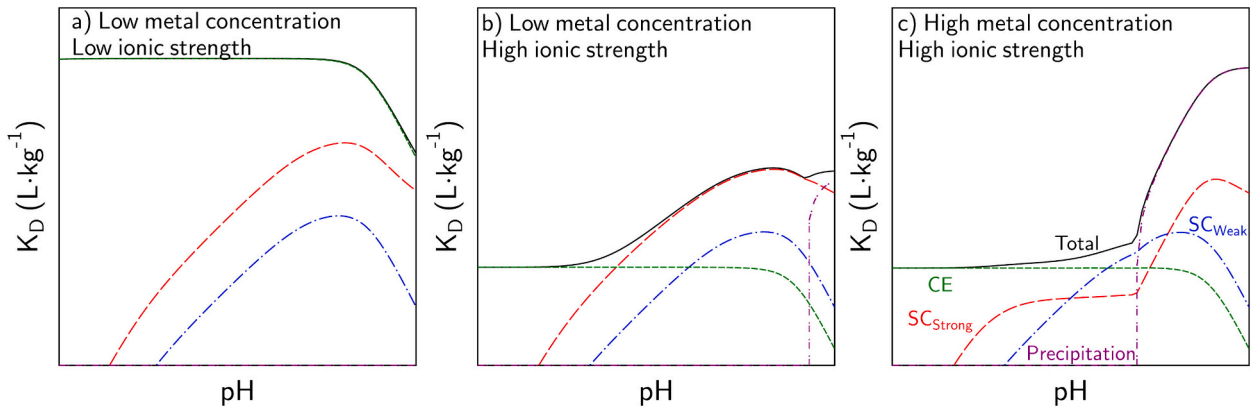

Fig. 1. Schematic representation of the influence of pH on the K_D value (plain black line) at low (e.g. 0.001) (a) and high ionic strength (e.g. 0.1) (b,c) for low (a,b) and high (c) divalent metal concentrations. Dashed lines are indicative of the contributions of cation exchange (CE, green), adsorption on strong sites (red), adsorption on weak sites (blue), and precipitation (purple) to the overall sorption. The breakdown of surface complexation sites into two categories, strong and weak sites, is arbitrary and must be seen as a simplification of the heterogeneity of adsorption sites. (For interpretation of the references to colour in this figure legend, the reader is referred to the web version of this article.)

capacity/lower affinity for the sorbates. Most of the data used to calibrate this model originates from the same research group at the Paul Scherrer Institute (see Table 1 for reactions and associated parameters). This research group used the same batch of montmorillonite samples and kept the same sample preparation procedure throughout the studies they published over more than twenty years, hence allowing them to build a consistent model to quantify the adsorption of numerous elements and their sorption competition. Two chief advantages of the 2SPNE SC/CE model are (1) its effectiveness in reproducing an extended range of adsorption data, and (2) its simplicity, which makes it easy to implement in geochemical speciation codes. This model has been used to predict the adsorption properties of clayey materials such as the MX80 bentonite and the Opalinus Clay (Bradbury and Baeyens, 2011; Marques Fernandes et al., 2015). All these criteria make the 2SPNE SC/CE model the ideal model to test the genericity of a surface complexation model and its parameters on a wider range of data obtained from the literature.

A fundamental criticism of the 2SPNE SC/CE model is its lack of electrostatic potential term associated with the surface complexation reaction, which departs from a distinctive property of clay mineral particles that is their electrostatic properties (Morel, 1997; Morel and Kraepiel, 1997; Kraepiel et al., 1999; Tournassat et al., 2013, 2016). Recently, multi-scale investigations of the clay mineral surface properties, which take into account the complexity of their surface structural properties, helped re-introducing an electrostatic term in montmorillonite surface complexation models (Tournassat et al., 2016, 2018; Orucoglu et al., 2018; Zhang et al., 2018; Liu et al., 2022; Gao et al., 2023). However, these models are not yet applicable to the same range of data that the 2SPNE SC/CE model can handle.

Tournassat et al. (2013) suggested that, despite its simplicity, the 2SPNE SC/CE model was over-parameterized. They demonstrated that a different non-electrostatic model could successfully fit the Ni and Zn adsorption data on montmorillonite with fewer parameters than the 2SPNE SC/CE model. Orucoglu et al. (2018) used the same approach to model Pb sorption onto montmorillonite and illite, which was further used to predict the adsorption of Pb onto a natural clayey rock from the Callovian-Oxfordian formation in Bure (France). For the present study, the goodness of fit (or prediction) is considered to be the ultimate criterion of the quality and usefulness of a model, and so, this "minimalist" model was extended and tested for other divalent metals and a wider range of data from the literature.

2.3. Data selection

Literature data were selected (Table 2) based on the availability of information about the types of divalent metallic cation and their concentration, the solid-to-liquid ratio, the type of background electrolyte, the ionic strength, the pH, and the type of clay mineral used in the experiments.

3. Methods

3.1. Geochemical code and thermodynamic database

Calculations were carried out using PHREEQC v3 (Parkhurst and Appelo, 2013) together with the ThermoChimie_PHREEQC_eDH_v9b0.dat database (https://www.thermochimie-tdb.com/) (Giffaut et al., 2014) to calculate the aqueous speciation and precipitation reactions. The activity coefficients were calculated using the Debye-Huckel equation. Four speciation reactions that were not specified in the ThermoChimie_PHREEQC_eDH_v9b0 database were taken from other databases (see Table S4 in supplementary information).

3.2. Modeling procedure

The two modeling approaches were used to quantify the adsorption of Ni^{2+}, Pb^{2+}, Mn^{2+}, Co^{2+}, $Cu^{2+}$and Cd^{2+}, at ionic strength ranging from 0.0001 to 0.1, in the presence of NaCl, $NaNO_3$ and $NaClO_4$ background electrolytes, at 25 ± 5 °C, as a function of pH, and as a function of sorbate equilibrium concentration (Table 2).

The adsorption parameters of the 2SPNE SC/CE model were directly taken from the reference studies (see references in Table 1), while those of the minimalist model were determined by a fitting procedure applied to a subset of data taken from Baeyens and Bradbury (1995) (Ni, Mn), Orucoglu et al. (2018) (Pb) and Akafia et al. (2011) (Cd, Co, Cu). Then the cation exchange capacities, selectivity coefficients, site types, their protolysis constants, and the surface complexation reactions were considered to be non-adjustable parameters in all calculations.

The (partial) dissolution of clay and accessory minerals (e.g. calcite or dolomite) is responsible for the presence of Ca and Mg in solution and in cation exchange position. Because Ca^{2+} and Mg^{2+} compete with the sorbates of interest on the cation exchange sites, it is important to take into account the Ca + Mg inventory in the calculations. When there is no information about the total extractable Ca and Mg inventory or their concentration in solution, it is thus necessary to estimate these quantities. Baeyens and Bradbury (1995) demonstrated that the purification process significantly decreases the aqueous and exchangeable Mg and Ca concentration in clay dispersions. These values may thus be strongly dependent on the sample origin of clay material type and of the applied

Table 1
Parameters of the 2SPNE SC/CE model and the minimalist model.

Cation Exchange	2SPNE-SC/CE model	Minimalist model
	Log K	Log K
$X^- + Na^+ = XNa$	0	0
$2X^- + Mg^{2+} = X_2Mg$	0.4[a]	0.6[e]
$2X^- + Ca^{2+} = X_2Ca$	0.4[a]	0.6[f]
$2X^- + Pb^{2+} = X_2Pb$	0.52[b]	0.6[e]
$2X^- + Cd^{2+} = X_2Cd$	0.45[c]	0.5[f]
$2X^- + Co^{2+} = X_2Co$	0.57[c]	0.6[f]
$2X^- + Ni^{2+} = X_2Ni$	0.5[c]	0.5[f]
$2X^- + Mn^{2+} = X_2Mn$	0.5[f]	0.5[f]
$2X^- + Cu^{2+} = X_2Cu$	0.5[f]	0.6[f]
First (Strong) Site -Protolysis reactions		
$>S_sOH = \geq S_sO^- + H^+$	−7.9[c]	−8.1[e]
$>S_sOH + H^+ = \geq S_sOH_2^+$	4.5[c]	Not Used
First (Strong) Site-SC Reactions		
$>S_sOH + Pb^{2+} = \geq S_sOPb^+ + H^+$	1[b]	0[e]
$>S_sOH + Pb^{2+} + H_2O = \geq S_sOPbOH + 2H^+$	−7.6[b]	Not Used
$>S_sOH + Cd^{2+} = \geq S_sOCd^+ + H^+$	−1[c]	−2.2[f]
$>S_sOH + Cd^{2+} + H_2O = \geq S_sOCdOH + 2H^+$	Not Used	−10.9[f]
$>S_sOH + Co^{2+} = \geq S_sOCo^+ + H^+$	−0.21[d]	−2.6[f]
$>S_sOH + Co^{2+} + H_2O = \geq S_sOCoOH + 2H^+$	Not Used	−10.5[f]
$>S_sOH + Ni^{2+} = \geq S_sONi^+ + H^+$	−0.6[c]	−1.6[f]
$>S_sOH + Ni^{2+} + H_2O = \geq S_sONiOH + 2H^+$	−10[c]	−12[f]
$>S_sOH + Ni^{2+} + 2H_2O = \geq S_sONi(OH)_2^- + 3H^+$	−20[c]	−20.4[f]
$>S_sOH + Mn^{2+} = \geq S_sOMn^+ + H^+$	−0.6[c]	−1.5[f]
$>S_sOH + Mn^{2+} + H_2O = \geq S_sOMnOH + 2H^+$	−11[c]	−12.3[f]
$>S_sOH + Cu^{2+} = \geq S_sOCu^+ + H^+$	0.94[d]	−0.4[f]
Second (Weak) Site-Protolysis reactions		
$>S_wOH = \geq S_wO^- + H^+$	−7.9[c]	Not Used
$>S_wOH + H^+ = \geq S_wOH_2^+$	4.5[c]	Not Used
Second (Weak) Site –SC Reactions		
$>S_wOH + Pb^{2+} = \geq S_wOPb^+ + H^+$	−1.5[b]	Not Used
$>S_wOH + Cd^{2+} = \geq S_wOCd^+ + H^+$	−3.7[d]	Not Used
$>S_wOH + Co^{2+} = \geq S_wOCo^+ + H^+$	−2.8[d]	Not Used
$>S_wOH + Ni^{2+} = \geq S_wONi^+ + H^+$	−3.3	Not Used
$>S_wOH + Mn^{2+} = \geq S_wOMn^+ + H^+$	−4.2[d]	Not Used
$>S_wOH + Cu^{2+} = \geq S_wOCu^+ + H^+$	−1.6[d]	Not Used
	Site density ($mol \bullet kg^{-1}$)	
First site	0.002[c]	0.02[f]
Second site	0.04[c]	Not Used
Cation exchange capacity (CEC)	0.87[c]	0.76[g]

[a] After Bradbury and Baeyens (2009c).
[b] Marques Fernandes and Baeyens (2019).
[c] Bradbury and Baeyens (2005a).
[d] LFER in Bradbury and Baeyens (2005a).
[e] Orucoglu et al. (2018).
[f] This study.
[g] Tournassat et al. (2004).

purification method, if any, carried out before the sorption experiment. Unfortunately, in most of the sorption experiments reported in the literature, the Mg and Ca concentrations in the solution and the solid phases are not reported, with the exception of data reported in Baeyens and Bradbury (1995) (110 $mmol_{Ca} \cdot kg_{clay}^{-1}$ and 270 $mmol_{Mg} \cdot kg_{clay}^{-1}$ were released in solution with the raw material; 11 $mmol_{Ca} \cdot kg^{-1}$ and 1.1 $mmol_{Mg} \cdot kg^{-1}$ were released in solution with the purified montmorillonite) and Gu et al. (2010) (110 $mmol_{Mg} \cdot kg_{clay}^{-1}$ were released in solution with the raw material). Hence, it was estimated that the Mg + Ca concentration was within the range of 0.07 $mol \cdot kg^{-1}$ to 0.58 $mol \cdot kg^{-1}$ depending on the applied purification process (Orucoglu et al., 2018). The estimated Mg + Ca concentrations, which were used in the 2SPNE SC/CE and minimalist model predictions, are given in Table S1.The precipitation of metal hydroxides and of carbonate minerals was taken into account using the solubility tabulated in the thermodynamic database.

Another factor that influences the adsorption efficiency is the competition with other metallic cations released in solution from the clayey materials. Baeyens and Bradbury (1995) measured Zn and Mn concentrations released in solution after severe acid dissolution at 0.8 and 1.6 $mmol \cdot kg^{-1}$ for raw montmorillonite and 0.8 and 0.4 $mmol \cdot kg^{-1}$ for purified montmorillonite respectively. Unlike the concentration of Ca^{2+} and Mg^{2+}, the concentration of naturally occurring metallic cations was not affected significantly by the montmorillonite purification process, indicating that Zn^{2+} and Mn^{2+} were likely desorbed from the clay mineral surfaces during the extraction procedure. The presence of these metallic cations decreases the effectiveness of the surface complexation of the investigated metallic cations because of sorption competition (Bradbury and Baeyens, 2005b; Chen et al., 2014a; Grangeon et al., 2015; Marques Fernandes and Baeyens, 2019; Montavon et al., 2020).

3.3. Statistical analysis of the results

The statistical analysis was carried out using R (R_Core_Team, 2020). The distribution of the measured $\log_{10} K_D$ values compared to the predicted $\log_{10} K_D$ values was analyzed with the Shapiro-Wilk normality test and the normal quantile-quantile (Q-Q) plot. The data is normally distributed if the probability of the Shapiro-Wilk test is bigger than or equal to 0.05. The Q-Q plots helped to visualize how well the datasets matched with the standard normal (Gaussian) distribution.

Spearman rank correlation (Spearman's rho) coefficients were used to describe the degree of correlation between predicted and measured data. Additionally, the Nash-Sutcliffe efficiency (NSE) test was used to determine the relative magnitude of the residual variance compared to the measured data variance using predicted and measured data (Nash and Sutcliffe, 1970; Moriasi et al., 2007). The NSE was calculated with the following equation.

$$NSE = 1 - \frac{\sum_1^n (X_i - Y_i)^2}{\sum_1^n (X_i - \overline{X})^2} \quad (1)$$

where X_i is $\log_{10}$(measured K_D), Y_i is $\log_{10}$(predicted K_D), $\overline{X}$ is the mean of $\log_{10}$(measured K_D). Recommended general performance ratings are given in Table S5 (Moriasi et al., 2007).

4. Results and discussion

4.1. Influence of the side reactions on sorption data

First, the modeling of data from Akafia et al. (2011) (Fig. 2a and d), and other publications (not shown) and relative to Ni^{2+} and Pb^{2+} sorption on montmorillonite was attempted using the 2SPNE SC/CE model, without consideration of possible sorption competition or possible precipitation of secondary phases, because no information was given relative to these phenomena in Akafia et al. (2011). In this configuration, the model had an apparent lack of predictive capability. Sorption data at pH < 6 were correctly reproduced for an ionic strength of 0.1 but were largely overestimated at lower ionic strength. At pH > 8, the model predicted a decrease in the K_D value and thus failed in reproducing the increase of sorption with pH. Cation exchange is the main mechanism responsible for sorption at low pH. Consequently, the mismatch between the prediction and the experimental data was the result of either a variation of the Na^+-Ni^{2+} and Na^+-Pb^{2+} selectivity coefficients with ionic strength, which, contrastingly, are kept fixed in the model, or the non-consideration of a competing cation in the system. Indeed, Orucoglu et al. (2018) showed that the clay material used by Akafia et al. (2011) contains Mg^{2+} and Ca^{2+} that compete with other cations for the exchanger sites. A contribution of 580 $mmol_{Ca+Mg} \cdot kg_{clay}^{-1}$ present initially in the clay material, decreased the predicted K_D down to

Table 2
Summary of the experimental conditions of sorption data available for divalent metallic cations in the literature.

Reference	Dataset number	Clay type	Clay preparation	S/L Ratio ($g \cdot L^{-1}$)	pH range	Ionic strength	Background electrolyte	Divalent metal	Metal loading ($mmol \cdot kg^{-1}$)	Temp. (°C)	Atmosphere
Akafia et al. (2011)	1	Mont. (SWy-2)	None	0.5	3–11	0.001–0.1	$NaNO_3$	Cd, Co, Cu, Ni, Pb	1–100	Room T	Ambient air
Baeyens and Bradbury (1997)	2	Na-SWy-1	1 M NaClO4 washing Acid treatment at pH 3.5	0.24, 1.1	2–10	0.03, 0.1	$NaClO_4$	Mn, Ni	0.03–172	Room T	Glove box $pCO_2 < 10^{-5.5}$ atm
Bogolepov (2009)	3	Natural Mont. from Cherkassy	Impurities removed	4	3–10	0.01–0.1	NaCl	Co(II)	50	Room T	Ambient air
Businelli et al. (2003)	4	Mont. (Upton, Wyoming	Na saturated, Removal of Carbonate (HCl) <2 μm freeze-dried	5	2–9	0.01-0.1	$NaNO_3$	Pb	100–400	23	Ambient air
Marques Fernandes and Baeyens (2019)	5	SWy-2 Mont. Na homoionic	< 0.5 μm, 1 M NaCl washing Treated at 0.1 M NaCl at pH 3.5 for 1 h	1.1–2.6	2–10	0.1	NaCl	Pb	0–426	Room T	Glove box $pCO_2 \leq 10^{-6}$ atm, $O_2 \leq 10^{-6}$ atm
Garcia-Miragaya and Page (1976)	6	Upton Mont.	< 2 μm	2.17	6.5–7	0.01–1	$NaClO_4$, NaCl	Cd	0.01–0.49	Room T	Ambient air
Ghayaza et al. (2011)	7	Swy-2 Mont.	< 2 μm Na saturated	10	5	0.04 0.01–0.001	NaCl Acetate	Pb	0.1–1000	Room T	Ambient air
Gu et al. (2010)	8	Mont. Wyoming	<2 μm fraction 0.5 M NaNO3 treated for 5 h	1.5	3 to 9	0.001–0.1	$NaNO_3$	Cd, Cu, Ni, Pb	32.5	25	Solution and tubes purged with Ar
Lothenbach et al. (1997)	9	Swy-1	< 2 μm, saturated with 1 M NaCl	2	4–10	0.1	NaC1 $NaClO_4$	Cd, Cu, Ni, Pb	50–500	Room T	Vessel purged with Ar
Zachara et al. (1993)	10	Na-Swy-1	< 2 μm Na saturated dialyzed freeze-dried	1	4–7	0.001–0.1	$NaClO_4$, $CaClO_4$	Cd	0.02–30	25	N_2 atmosphere
Marcussen et al. (2009)	11	Swy-2	< 2 μm, saturated with 0.5 M $NaNO_3$	2	4–7	0.01	$NaNO_3$	Ni	0.25–8.5	20	Ambient air
Morton et al. (2001)	12	Cheoto Mont.	<2 μm fraction removal of Fe oxide, carbonate, & organic matter	0.5	2.5–11.5	0.02–0.1	$NaNO_3$	Cu	16–200	30	Ambient air
Strawn and Sparks (1999)	13	Swy-2 Mont.	< 2 μm, Na saturated removal of carbonate & organic matter	10	4–8	0.006, 0.1	$NaClO_4$	Pb	200	25	Glove box
Green-Pedersen and Pind (2000)	14	Mont. (WY, USA)	None	0.04, 0.07	6.9–8.1	0.001	$NaNO_3$	Ni	12.5–155	25	Ambient air
Shao et al. (2009)	15	MX-80	None	0.4	2–10	0.001–0.1	$NaClO_4$, NaCl	Ni	425	25	Under N_2 conditions
Chen and Dong (2013)	16	Mont. (Zhejiang, China)	None	0.5	4–12	0.001–0.1	$NaClO_4$,	Ni	340	20	Ambient air
Orucoglu et al. (2018)	17	MX-80	< 2 μm, Na saturated Removal of carbonate & organic matter	1	3–9	0.025–0.1	NaCl	Pb	1–50	20	Ambient air

(*continued on next page*)

Table 2 (*continued*)

Reference	Dataset number	Clay type	Clay preparation	S/L Ratio ($g \cdot L^{-1}$)	pH range	Ionic strength	Background electrolyte	Divalent metal	Metal loading ($mmol \cdot kg^{-1}$)	Temp. (°C)	Atmosphere
Tertre et al. (2005)	18	MX-80 Bentonite	Removal of carbonate decantation for other impurities 0.2–2 μm fraction saturated with 1 M NaCl	2.5	2–10	0.025–0.5	NaCl	Ni	0.68	25	Ambient air
Yu et al. (2016)	19	Mont. (Zhejiang, China)	None	0.5	3–12	0.001–0.1	$NaNO_3$	Ni	39–403	25	Ambient air
Chen et al. (2016)	20	Mont. (Zhejiang, China)	None	0.6	2–10	0.001–0.1	$NaClO_4$,	Ni	95–420	20	Ambient air
Wang et al. (2009)	21	GMZ Bentonite (Mongolia)	< 53 μm, saturated with 1 M NaCl	0.5	2–12	0.001–0.1	$NaNO_3$	Pb	58–212	20	Ambient air
Hu et al. (2018)	22	Mont. (Mongolia)	< 2 μm	1	3.10	0.0001–0.01	NaCl	Co	14–170	20	Ambient air
Yang et al. (2010)	23	Mont. (Zhejiang, China)	< 53 μm, saturated with 1 M NaCl	0.5	2–12	0.001–0.1	$NaClO_4$,	Pb	29–348	25	Ambient air
Wen et al. (2011)	24	Mont. (Zhejiang, China)	None	0.5	1–12	0.001–0.1	$NaNO_3$, NaCl,	Co	167–934	20	Ambient air
Hu and Tan (2012)	25	Mont. (Zhejiang, China)	None	0.7	2–12	0.001–0.1	$NaNO_3$	Ni	89–1334	25	Ambient air
Wu et al. (2011)	26	Mont. (Zhejiang, China)	None	0.6	2–11	0.001–0.1	$NaClO_4$,	Cu	14–418	25	Ambient air
Li et al. (2009)	27	GMZ Bentonite (Mongolia)	< 53 μm, saturated with 1 M NaCl	0.5	3–11	0.001–0.1	$NaNO_3$	Cu	120–700	20	Ambient air

C: Clay; BE: Background electrolyte, Me: Metal.

values in remarkable agreement with the experimental values. (Fig. 2b and e). The chosen Mg and Ca total concentration was consistent with measurements carried out in studies of raw bentonite dissolution (Baeyens and Bradbury, 1995; Gu et al., 2010). This result highlights the need to quantify and provide the solution composition associated to sorption experiments for them to be interpretable. At high pH, the model prediction can be reconciled with the observed K_D values by considering the precipitation of nickel hydroxide, $Ni(OH)_2$, and hydrocerussite, $Pb_3(CO_3)_2(OH)_2$, at thermodynamic equilibrium with a dissolved inorganic carbon (DIC) concentration of 0.25 mM (Orucoglu et al., 2018). Total or dissolved inorganic carbon concentrations are usually, and unfortunately, not provided in the clay sorption literature. Alkalinity measurements at pH ranging from ~5.5 to 9 were provided by Orucoglu et al. (2018). In that study, it was observed that the samples had alkalinity values within the range of 0.17–0.31 $meq \bullet L^{-1}$ in the presence or absence of clay. These alkalinity values corresponded to calculated DIC concentrations of ~0.25 $mmol \bullet L^{-1}$ that were consistent with a near equilibrium of the stock solutions and dispersions with the atmospheric CO_2 partial pressure ($\log pCO_2 \sim -3.5$) before the adsorption experiments at pH 7–8. Consequently, the same DIC concentration was considered for the model predictions in the present study. Doing so, the quality of the model predictions improved markedly (Fig. 2), thus showing clearly that the discrepancies between the model predictions and the experimental data may not be related to flaws in the surface complexation model parameterizations, but rather to an incomplete consideration of true experimental conditions, and thus the incompleteness of the modeled reactions that are necessary to interpret the data (competition effect, precipitation).

4.2. Comparison of the predictions of the minimalist and the 2SPNE SC/CE models for a single dataset

The minimalist modeling approach was first tested with the Pb^{2+}, Ni^{2+}, Co^{2+}, Cu^{2+}, and Cd^{2+} sorption data on montmorillonite from Akafia et al. (2011), which are available as a function of pH at three different ionic strengths and two different metal concentrations (50 and 5 μM) (Fig. 3 and Fig. S1). In parallel, predictions were made with the 2SPNE SC/CE model. The Ca + Mg exchange correction and the consideration of precipitation of metal hydroxides and carbonates highlighted in the previous paragraph were taken into account. The same correction parameters were applied to both models. At a total metal concentration of 5 μM (Fig. S1), the 2SPNE SC/CE model predictions were in good agreement with Co^{2+} sorption results. However, the sorption of Pb^{2+}, Ni^{2+}, Cu^{2+}, and Cd^{2+} was underestimated, especially at an ionic strength of 0.1. The minimalist model made it possible to better fit most of the data despite its lesser number of parameters (Fig. 3 and Fig. S2). The two models reproduced equally well the experimental data at a total metallic cation concentration of 50 μM (Fig. 3). At 5 μM, the metal-to-solid ratio was 10 $mmol \bullet kg^{-1}$, which is five times higher than the total site capacity of the strong sites considered in the 2SPNE SC/CE model (2 $mmol \bullet kg^{-1}$). The influence of the strong sites on the adsorption prediction is thus negligible compared to that of the weak sites, which, in turn, explains why a minimalist model, with only one surface complexation site, but with adjusted parameters,

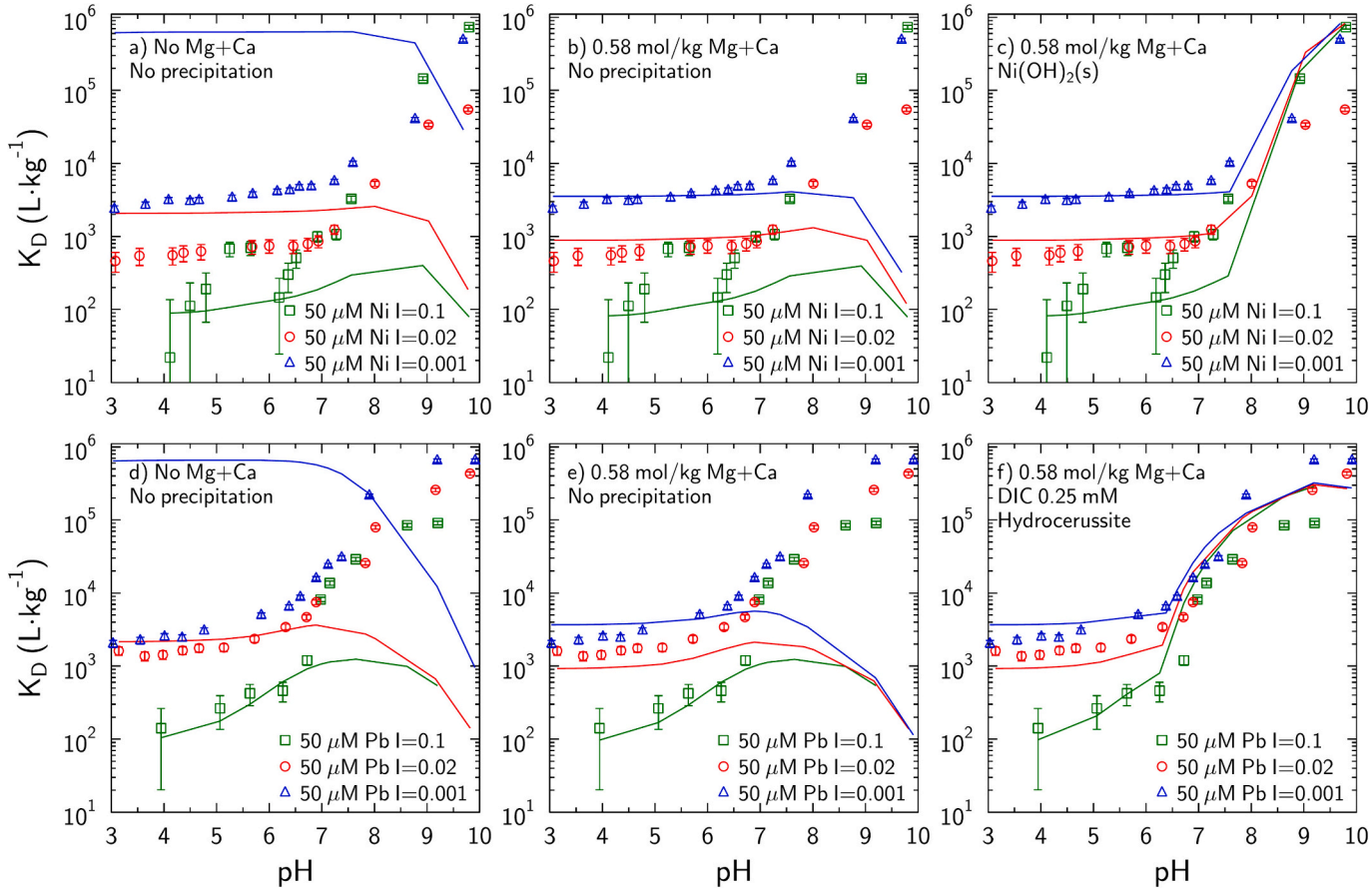

Fig. 2. Prediction of Ni^{2+} (a-c) and Pb^{2+} (d-f) sorption using the 2SPNE SC/CE model. a and d: no correction; b and e: consideration of the presence of exchangeable Ca + Mg in the clay material; c and f: same as b and e with additional consideration of $Ni(OH)_2$ and hydrocerussite precipitation at thermodynamic equilibrium.

was able to fit the data better. At 50 μM total metal concentration, the metal-to-solid ratio was 100 mmol•kg^{-1}, which is 2.5 times higher than the total site capacity of the weak sites in the 2SPNE SC/CE model, and 5 times higher than the surface complexation site capacity in the minimalist model. Hence, most of the sorption signal is dominated by cation exchange and precipitation processes, which, in turn, explains why the 2SPNE SC/CE and minimalist models performed equally well. The 2SPNE SC/CE model parameters have been calibrated with experimental data that were mostly obtained using <2 μm montmorillonite particles purified from the SWy-1 material of the Source Clay repository (Bradbury and Baeyens, 2005b). Constractingly, the data from Akafia et al. (2011) were obtained using a raw SWy-2 material. Thus, the discrepancy observed at 5 μM total metal concentration between the measured K_D values and the values predicted with the 2SPNE SC/CE model may be attributed to a difference in clay material properties or to an imprecise parameterization of the adsorption properties for the weak sites. While the former reason cannot be excluded, the surface complexation constants of Cd^{2+}, Co^{2+}, Cu^{2+} and Mn^{2+} sorption on weak sites (Table 1) were estimated from the LFER provided in Bradbury and Baeyens (2005a), thus pointing out the uncertainties related to the use of this relationship.

4.3. Comparison of the 2SPNE SC/CE model prediction with data from 27 literature references

For each of the datasets available in Table 2, the modeled K_D values were compared to the measured values, taking into account, or not, the presence of Ca + Mg, and the precipitation of metal hydroxide. The dataset was split into 3 pH domains in which cation exchange, surface complexation, and precipitation were the main mechanisms for the observed sorption, respectively. These three pH domains were 2–5, 5–8, and 8–12 for Ni, Cd, and Co; 2–4, 4–6.5, and 6.5–12 for Pb and 2–4, 4–6, and 6–12 for Cu. In the absence of correction, the 2SPNE SC/CE model failed to predict the data gathered from the literature (Fig. 4, and Figs. S3(a-c), S6 to S8(a-c)), with differences up to 4 orders of magnitude in K_D values. The largest differences were observed in the low and high pH intervals, which echoes the necessity to consider additional processes in these pH ranges as pointed out in the analysis of Akafia et al. (2011) data.

When considering the presence of Ca + Mg in the clay material, the 2SPNE SC/CE model predictions improved significantly in the low pH range, but also in the middle pH range for experiments conducted at low ionic strength values (Fig. 5, Figs. S4(a, b) and S6(d, e) to S8(d, e)).

At last, the 2SPNE SC/CE model predictions improved again significantly when metal hydroxide precipitation was considered (Fig. 6, Figs. S5(c) and S6(f) to S8(f)). Most of the log K_D values were predicted within a ± 1 interval with some outlier data originating from a small number of literature references.

The nature of the precipitates at high pH and high metallic cation concentration cannot be deduced from the aqueous concentrations and their identification relies on diffractometric and spectroscopic studies. Surface precipitation during metal sorption by clay minerals and oxides has been investigated for Ni, Co, Cu, Cd, and Pb cations (O'Day et al., 1994; Scheidegger et al., 1998; Chen and Hayes, 1999; Ford et al., 1999; Scheinost and Sparks, 2000; Morton et al., 2001; Hyun and Hayes, 2004; Gräfe et al., 2007; Yang et al., 2015; Woodward et al., 2018). Ni precipitates onto oxide and clay mineral surfaces include turbostratic α-type metal hydroxide, layered double hydroxide (LDH), as well as 1:1 or 2:1 phyllosilicates (Scheidegger et al., 1996; Ford et al., 1999; Elzinga and Sparks, 2001). Similar observations were done with Co (O'Day et al.,

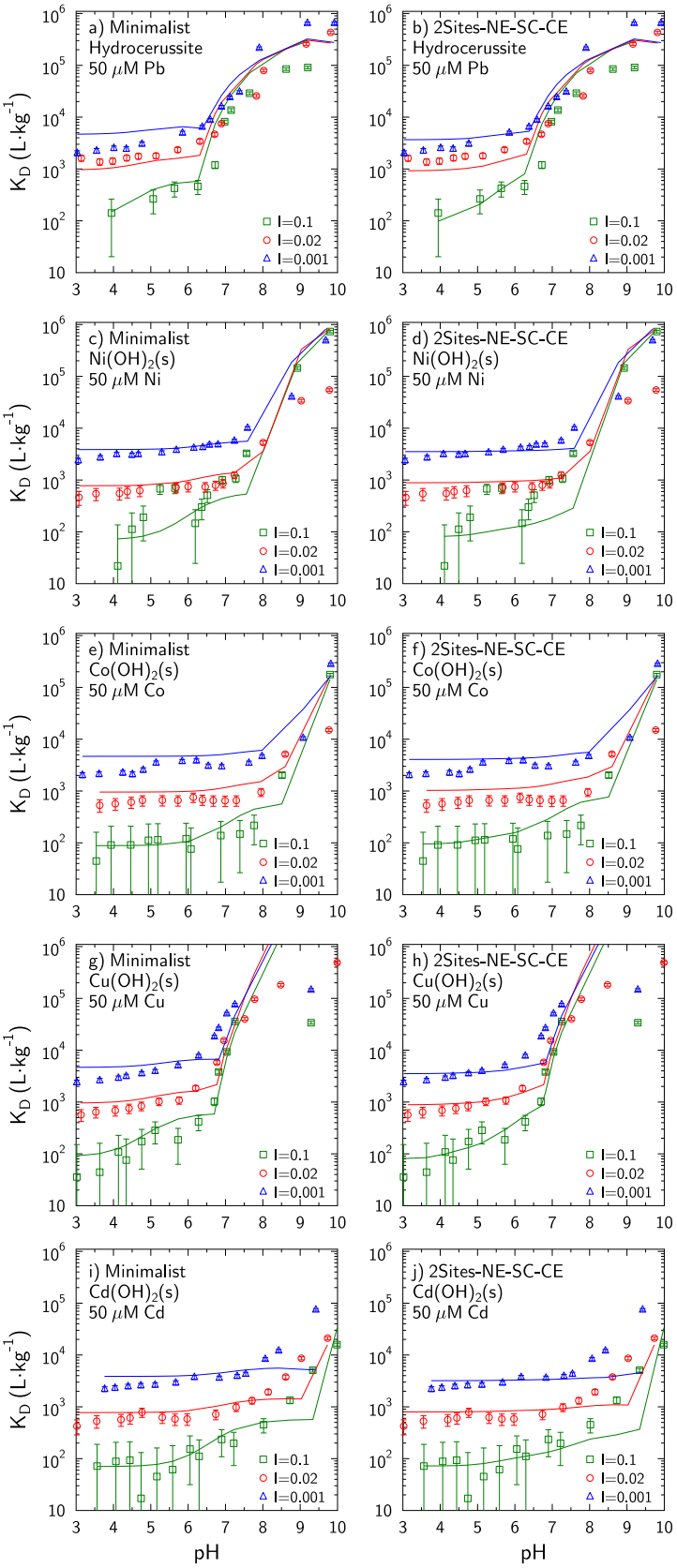

Fig. 3. Modeling of Pb^{2+}, Ni^{2+}, Co^{2+}, Cu^{2+}, and Cd^{2+} sorption data from Akafia et al. (2011) using the minimalist (first column) and the 2SPNE SC/CE (second column) models in the presence of 50 μM of metallic cation. Experimental conditions are available in the inner captions of the figure.

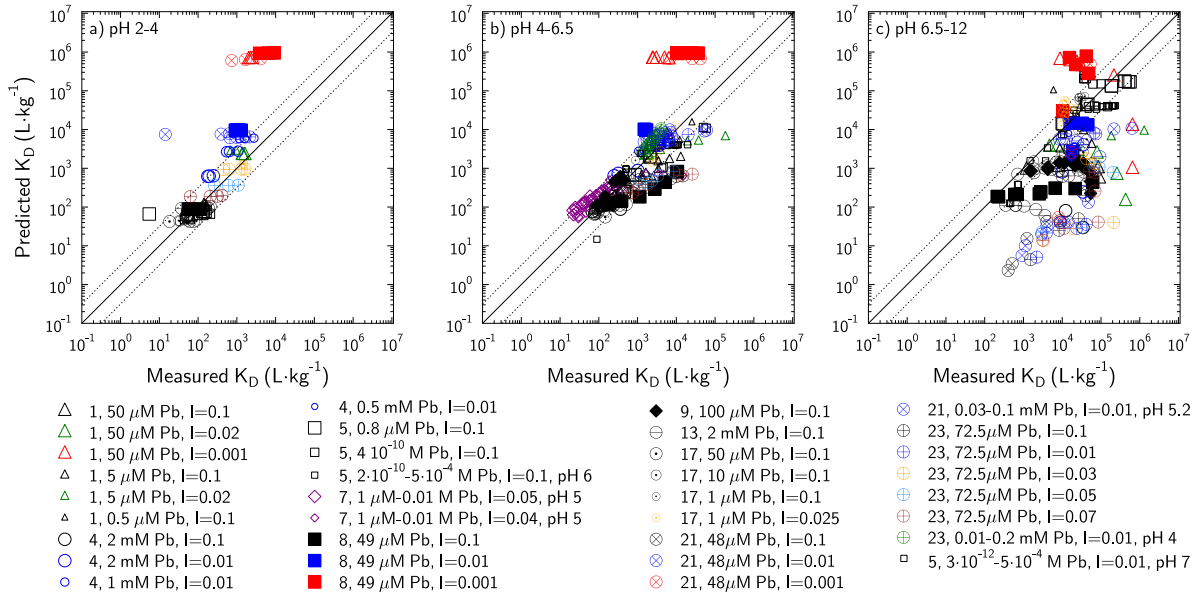

Fig. 4. Comparison of measured K_D values with values predicted with the 2SPNE SC/CE model for Pb (d-f) in three different pH ranges without corrections. The plain line shows the 1:1 relationship between the predicted and the measured K_D. The dashed lines are indicative of an ±0.5 difference in log K_D values. Symbols and numbers in the inner caption point to the references listed in Table 2.

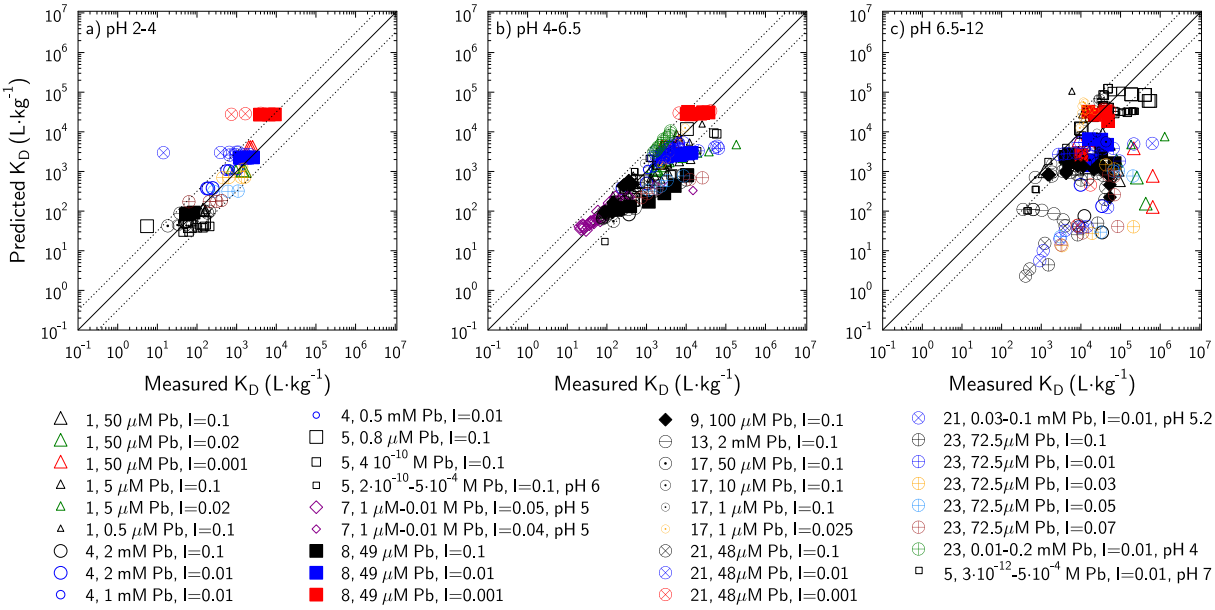

Fig. 5. Comparison of measured K_D values with values predicted with the 2SPNE SC/CE model for Pb (a-c) in three different pH ranges with the consideration of Ca + Mg concentration correction. The plain line shows the 1:1 relationship between the predicted and the measured K_D. The dashed lines are indicative of an ±0.5 difference in log K_D values. Symbols and numbers in the inner caption point to the references listed in Table 2.

1994; Papelis and Hayes, 1996; Chen and Hayes, 1999; Scheinost and Sparks, 2000). Carbonated minerals may also precipitate such as $Cu_2(OH)_2CO_3$(s) (Du et al., 1997), $CdCO_3$ (Papelis et al., 1995; Vasconcelos et al., 2008), $PbCO_3$ and $Pb3(OH)_2(CO3)$(Marani et al., 1995; Echeverría et al., 2005). The solubility of most of these phases, as well as the thermodynamics of surface precipitation, which may differ from that of homogeneous nucleation, is however not well documented (Scheinost and Sparks, 2000; Centofanti et al., 2012), and thus not available in geochemical codes and their thermodynamic databases. Furthermore, uncertainties related to the surface precipitation model and its initiation as a function of the solubility limit are additional reasons that could explain the discrepancies between the data and the model predictions at high pH values. Sorption experiments are also commonly carried out over a short equilibration time, and the system may not reach a thermodynamic equilibrium with precipitated minerals. For these reasons, an accurate prediction of sorption data at high pH and high metallic cation concentration is not, currently, a realistic objective. Consequently, no further attempts were made to reduce the discrepancies between measured and modeled K_D values in these conditions.

4.4. Comparison of the minimalist model results with data from 27 literature references

The minimalist model was successful in reproducing the dataset (Fig. 7, and Figs. S9 to S12). The agreement between the data and the model was further evaluated using statistical analysis. Statistical

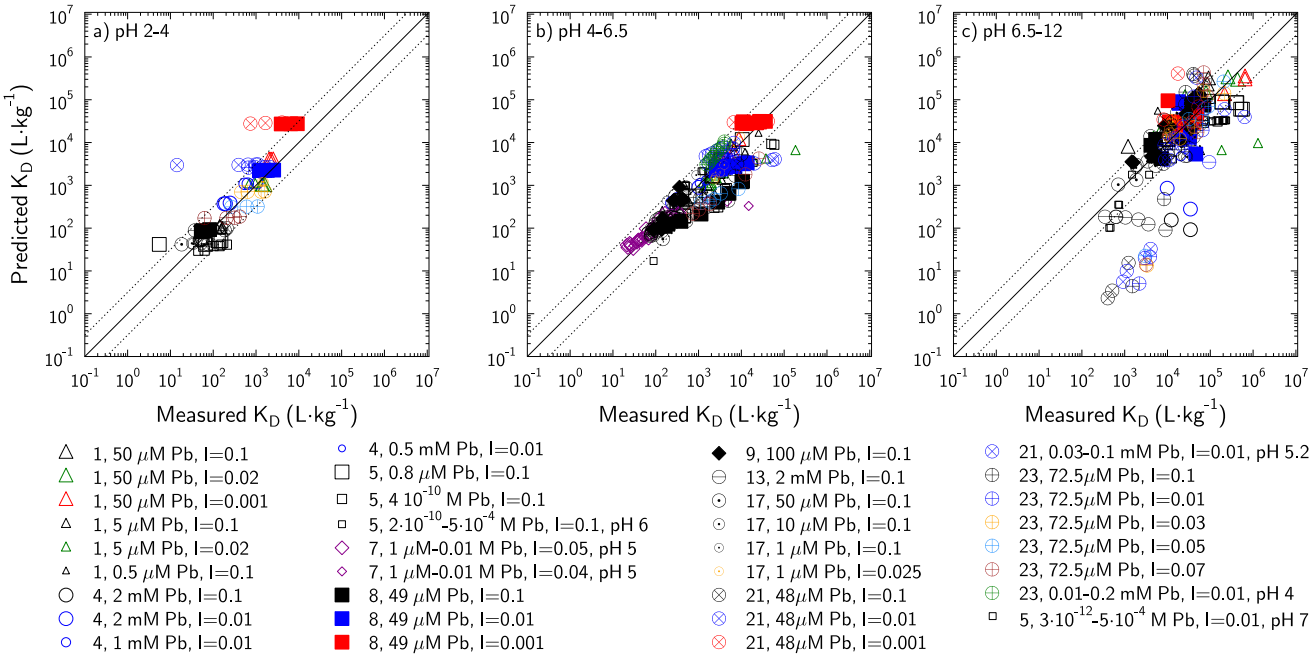

Fig. 6. Comparison of measured K_D values with values predicted with the 2SPNE SC/CE model for Pb (a-c) in three different pH ranges with the consideration of corrections related to the Ca + Mg concentration to the precipitation of metal hydroxides at high pH (Hydrocerussite). The plain line shows the 1:1 relationship between the predicted and the measured K_D. The dashed lines are indicative of an ±0.5 difference in log K_D values. The colors of the symbols are representative of the ionic strength. Symbols and numbers in the inner caption point to the references listed in Table 2.

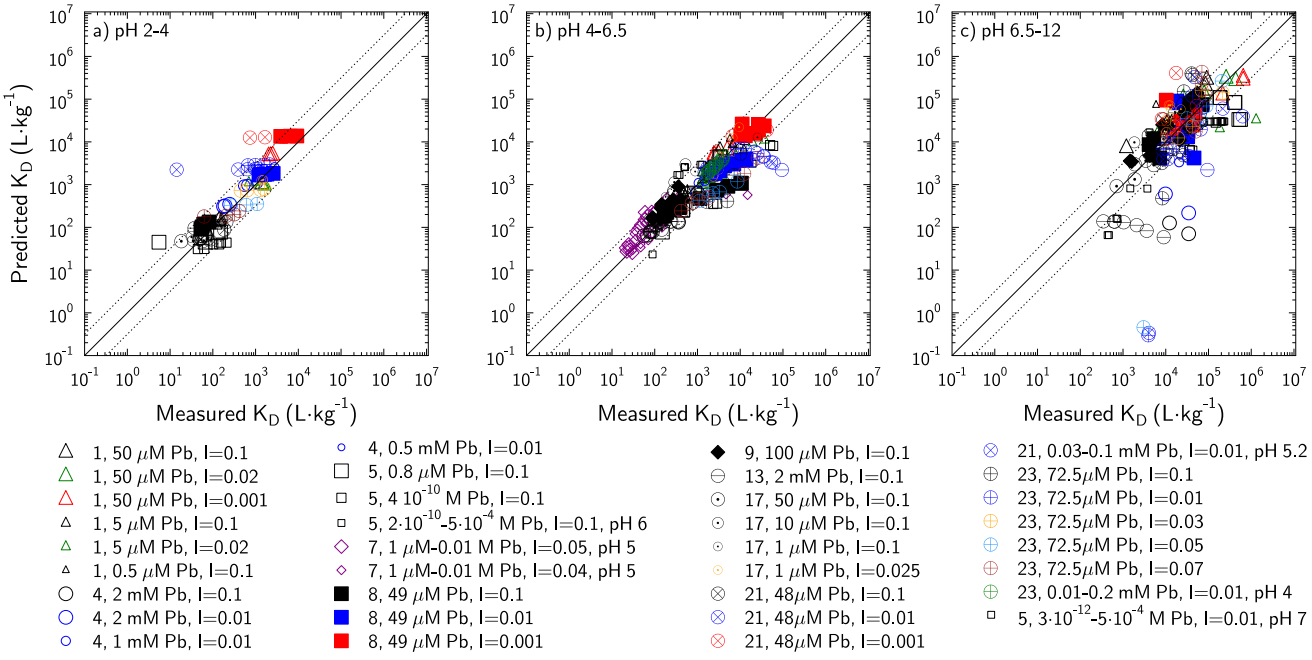

Fig. 7. Comparison of measured K_D values with values modeled with the minimalist approach for Pb (a-c) in three different pH ranges with the consideration of corrections related to the Ca + Mg concentration to the precipitation of metal hydroxides at high pH (Hydrocerussite). The plain line shows the 1:1 relationship between the predicted and the measured K_D. The dashed lines are indicative of an ±0.5 difference in log K_D values. Symbols and numbers in the inner caption point to the references listed in Table 2.

analyses were carried out in the full pH range (2−12) and the low, middle, and high pH sub-ranges. Q-Q plots showed that 4 outliers in the Pb dataset and one outlier in the Co dataset have high leverage values and these values were removed from the analysis. Ni, Cd, Co, and Cu data had at least one pH range with a normal distribution, while Pb data had a non-normal distribution whatever the considered pH range. On the other hand, most of the predicted $\log_{10} K_D$ datasets had a non-normal distribution (Table S2).

Because of the normal distributions of the predicted $\log_{10} K_D$ datasets, Spearman's rho correlation coefficient calculations were carried out to explore the relationships between the measured and the predicted data (Table S3). Additionally, Nash-Sutcliffe efficiency (NSE) performance calculations were carried out (Table 3) to investigate the goodness of fit between simulated results and observed measurements

Table 3
NSE performance calculation results.

		Full pH range	Low pH range	Middle pH range	High pH range
		Ni sorption			
2SPNE SC/CE model	No correction	−0.63	−1.47	−0.49	−6.23
	Ca + Mg correction	−0.11	0.49	0.47	−6.36
	Ca + Mg correction and mineral precipitation	0.55	0.49	0.53	−1.05
Minimalist	Ca + Mg correction and mineral precipitation	0.58	0.60	0.55	−0.98
		Pb sorption			
2SPNE SC/CE model	No correction	0.01	−0.91	0.46	−2.85
	Ca + Mg correction	0.15	0.48	0.73	−3.00
	Ca + Mg correction and mineral precipitation	0.64	0.48	0.77	−0.38
Minimalist	Ca + Mg correction and mineral precipitation	0.26	0.61	0.80	−2.56
		Cd sorption			
2SPNE SC/CE model	Ca + Mg correction and mineral precipitation	0.70	0.81	0.81	−1.98
Minimalist	Ca + Mg correction and mineral precipitation	0.74	0.89	0.75	−0.86
		Co sorption			
2SPNE SC/CE model	Ca + Mg correction and mineral precipitation	0.72	0.60	0.64	0.17
Minimalist	Ca + Mg correction and mineral precipitation	0.61	0.66	−0.05	−0.01
		Cu sorption			
2SPNE SC/CE model	Ca + Mg correction and mineral precipitation	−0.18	0.64	0.60	−2.50
Minimalist	Ca + Mg correction and mineral precipitation	−0.16	0.70	0.58	−2.46

(Legates and McCabe, 1999). NSE performances and correlation coefficients evidenced the improvement of the data-model agreement with the consideration of Ca + Mg and mineral precipitation corrections. Doing so, a satisfactory to a very good agreement was always reached for the low and middle pH ranges, while the high pH range showed unsatisfactory, albeit improved, agreement. The reasons for these remaining discrepencies have been discussed in the previous section. These calculations showed also surprisingly that a better performance was often achieved with the minimalist model than with the 2SPNE SC/CE model. At least three non-mutually exclusive explanations can be put forward to explain this counter-intuitive finding. First, the minimalist approach was optimized with a fitting procedure, thus explaining its good overall agreement with the data, while the 2SPNE SC/CE model was used "out of the box" to predict the experimental results of studies that were not used to calibrate its parameters. Second, a minor part of the dataset deals with metal-to-clay loading less than or in the order of magnitude of 2 mmol•kg^{-1}. Consequently, for most of the dataset, the influence of the strong sites on the total sorption is outsized by that of the weak sites and the exchange and precipitation processes. Hence, the calibration of the weak sites' properties in the 2SPNE SC/CE model is more important than that of the strong sites. Most of the weak sites' properties in the 2SPNE SC/CE model were not obtained from experimental data fitting, but rather from the LFER relationship from Bradbury and Baeyens (2005a) (Table 1). The analysis performed in this study shows that a reappraisal of this LFER is necessary for the weak sites. It is worth noting that Bradbury and Baeyens (2005a) mentioned that "the confidence in the correlation in LFERs between the [weak sites] surface complexation constants and hydrolysis constants is not as high as in the case of the strong sites".

4.5. Implication for the prediction of metal sorption in clay-based systems

The modeling of sorption in the framework of radioactive waste repository performance assessment deals with very low equilibrium aqueous concentrations of radionuclides, which correspond to conditions for which strong sites should be the main contributors to the overall sorption. However, the existence of strong sites in raw bentonites or the smectite components of natural clay rock samples is far from certain, and therefore, their significant contribution to the overall sorption in natural and engineered systems seems questionable. For example, Chen et al. (2014a) showed that the 2SPNE SC/CE model overestimated Ni^{2+} sorption on the clay fraction (< 2 μm) of Callovian-Oxfordian clay-rock samples, and that only one surface complexation site was necessary to fit the data. Their site had adsorption properties similar to that of weak sites in the present study. Montavon et al. (2020) confirmed these findings by studying the distribution ratio of natural Ni^{2+} between the aqueous pore solution and the mineral surfaces present in the Callovian-Oxfordian clayey formation. Tournassat et al. (2013) showed also that data of Ni^{2+} sorption on purified MX80 samples from Tertre et al. (2005) were not in agreement with the presence of reacting strong sites. Using a bottom-up approach with their 2SPNE SC/CE model, Bradbury and Baeyens (2011) needed to cancel the reactivity of strong sites to explain the Ni^{2+} sorption properties of MX80 bentonite and also Opalinus clay. To do so, they invoked a competition process with aqueous Fe^{2+} and Mn^{2+}, thereby blocking the access of Ni^{2+} to the strong sites. On the one hand, it remains unclear whether the absence of strong site reactivity in many datasets reported in the literature is due to the absence of strong sites or to the influence of cations competition between sorbents for adsorption to the site. The competition process between divalent cations is now well documented (Bradbury and Baeyens, 2005b; Soltermann et al., 2013; Marques Fernandes and Baeyens, 2019; Orucoglu et al., 2022), and measurements of pore water composition in clay rocks have assessed the presence of competing divalent at sufficient concentration to cancel the strong site contribution to radionuclide adsorption (Grangeon et al., 2015; Montavon et al., 2020). Additional complexity in quantifying the role of strong sites in clay sorption processes, and in particular competition effects, arises from the fact that the crystallographic nature of the strong site differs depending on the ion considered. For example, Zn^{2+} and Ni^{2+} sorb as a mixture of surface complexes bound to cis-vacant-like (cv-like) and trans-vacant-like (tv_like) edge sites, Fe preferentially sorbs at tv-like edge sites, and Am sorbs on the {010} and {110} edge faces by binding to three Al(O, OH)$_6$ (Dähn et al., 2003, 2011; Marques Fernandes et al., 2016). Hence, even the assumption of a unique "strong site" could be debated. Consequently, whatever the origin of the variability in the reactivity of strong sites reported in the literature, their consideration in performance evaluation studies may lead to an overestimation of the sorption efficiency of clay barriers.

The scattering of the literature data that correspond to weak sites' reactivity, i.e. data falling in the middle pH range, may be indicative of natural variability or of experimental biases. It is also certainly representative of the expected accuracy of a blind bottom-up approach used to predict the sorption properties of natural samples based on their clay mineralogical content and the in situ pore water composition. The present analysis shows that the accuracy of the log K_D value is not better than ±1 log unit.

5. Conclusions

Predicting the retention of divalent metals by montmorillonite is a key issue for performance assessment analysis in the context of waste disposal in clayey rocks and/or engineered barriers. In this study, a detailed analysis of literature data on divalent metal sorption by purified montmorillonite or montmorillonite-rich materials was carried out. The 2SPNE SC/CE model and the "minimalist" model were used to model data originating from 21 different literature studies.

This study showed that sorption data of divalent metal available in the literature must be corrected from two side reactions before being interpreted in the framework of a surface complexation model. First, the competition of the divalent metallic cations with aqueous Ca^{2+} and Mg^{2+} must be considered properly for cation exchange sites. Aqueous and exchanged Ca^{2+} and Mg^{2+} originate from the dissolution of montmorillonite (Mg^{2+}) and of the accessory minerals such as calcite and dolomite. The information about Ca^{2+} and Mg^{2+} concentration measurements is often missing, which prevents accurate modeling of sorption data at low ionic strength. Second, the precipitation of solids phases at high pH, which incorporate the divalent metallic cations of interest, renders experimental data meaningless for the calibration of surface complexation parameters at high pH. Measurements of an extended set of aqueous concentrations, including dissolved organic carbon, Si, and Al, would certainly help to better constrain the modeling of precipitation processes at high pH.

At last, this modeling analysis shows that without sorption data obtained on samples truly representative of the smectitic material of interest, the log K_D value of a divalent metallic cation cannot be predicted with an accuracy better than ± 1 log unit while using generic surface complexation model parameters. If a higher level of prediction is needed, experimental data obtained directly on the system of interest remains necessary. Furthermore, the consideration of most reactive sites, the strong sites, which have been characterized only on some specific montmorillonite samples may lead to a strong overestimation of K_D values in models predicting divalent metal behaviors in natural conditions on the basis of generic surface complexation models.

CRediT authorship contribution statement

Esra Orucoglu: Writing – review & editing, Writing – original draft, Validation, Methodology, Investigation, Formal analysis, Conceptualization. **Sylvain Grangeon:** Writing – review & editing, Writing – original draft, Validation, Methodology, Investigation, Formal analysis, Conceptualization. **Jean-Charles Robinet:** Writing – review & editing, Validation, Supervision, Resources, Project administration, Funding acquisition, Conceptualization. **Benoît Madé:** Writing – review & editing, Validation, Supervision, Resources, Project administration, Funding acquisition, Conceptualization. **Christophe Tournassat:** Writing – review & editing, Writing – original draft, Validation, Supervision, Resources, Project administration, Methodology, Investigation, Formal analysis, Conceptualization.

Declaration of competing interest

The authors declare that they have no known competing financial interests or personal relationships that could have appeared to influence the work reported in this paper.

Data availability

The sorption data used in this study were collected from the literature. All data sources are listed in the manuscript and supplementary file.

Acknowledgment

This work was supported by the French Radioactive Waste Management Agency (Andra) as part of the Andra-BRGM scientific partnership (CTEC project). CT acknowledges a grant overseen by the French National Research Agency (ANR) as part of the "Investissements d'Avenir" Programme LabEx VOLTAIRE, 10-LABX-0100.

Appendix A. Supplementary data

Supplementary data to this article can be found online at https://doi.org/10.1016/j.clay.2024.107569.

References

Akafia, M.M., Reich, T.J., Koretsky, C.M., 2011. Assessing Cd, Co, Cu, Ni, and Pb sorption on montmorillonite using surface complexation models. Appl. Geochem. 26, 154–157.
Altmann, S., Tournassat, C., Goutelard, F., Parneix, J.-C., Gimmi, T., Maes, N., 2012. Diffusion-driven transport in clayrock formations. Appl. Geochem. 27, 463–478.
Baeyens, B., Bradbury, M.H., 1995. A Quantitative Mechanistic Description of Ni, Zn and ca Sorption on Na-Montmorillonite. Part I: Physico-Chemical Characterisation and Titration Measurements. Paul Scherrer Institut (PSI), Villigen.
Baeyens, B., Bradbury, M.H., 1997. A mechanistic description of Ni and Zn sorption on Na-montmorillonite. Part I: Titration and sorption measurements. J. Contam. Hydrol. 27, 199–222.
Barbier, F., Duc, G., Petit-Ramel, M., 2000. Adsorption of lead and cadmium ions from aqueous solution to the montmorillonite/water interface. Colloids and Surf. A-Physicochem. Engineer. Aspects 166, 153–159.
Bardelli, F., Mondelli, C., Didier, M., Vitillo, J.G., Cavicchia, D.R., Robinet, J.-C., Leone, L., Charlet, L., 2014. Hydrogen uptake and diffusion in Callovo-Oxfordian clay rock for nuclear waste disposal technology. Appl. Geochem. 49, 168–177.
Beaucaire, C., Tertre, E., Ferrage, E., Grenut, B., Pronier, S., Madé, B., 2012. A thermodynamic model for the prediction of pore water composition of clayey rock at 25 and 80°C – Comparison with results from hydrothermal alteration experiments. Chem. Geol. 334, 62–76.
Bogolepov, A.A., 2009. Simulation of U(VI) and Co(II) sorption on montmorillonite. In: Radiochemistry (Moscow, Russian Federation)(Translation of Radiokhimiya), 51, pp. 96–103.
Bradbury, M.H., Baeyens, B., 1997. A mechanistic description of Ni and Zn sorption on Na-montmorillonite. Part II: modeling. J. Contam. Hydrol. 27, 223–248.
Bradbury, M.H., Baeyens, B., 1999. Modeling the sorption of Zn and Ni on Ca-montmorillonite. Geochim. Cosmochim. Acta 63, 325–336.
Bradbury, M.H., Baeyens, B., 2000. A generalised sorption model for the concentration dependent uptake of caesium by argillaceous rocksbae. J. Contam. Hydrol. 42, 141–163.
Bradbury, M.H., Baeyens, B., 2002. Sorption of Eu on Na- and Ca-montmorillonites: experimental investigations and modeling with cation exchange and surface complexation. Geochim. Cosmochim. Acta 66, 2325–2334.
Bradbury, M.H., Baeyens, B., 2005a. Modelling the sorption of Mn(II), Co(II), Ni(II), Zn (II), Cd(II), Eu(III), Am(III), Sn(IV), Th(IV), Np(V) and U(VI) on montmorillonite: Linear free energy relationships and estimates of surface binding constants for some selected heavy metals and actinides. Geochim. Cosmochim. Acta 69, 875–892.
Bradbury, M.H., Baeyens, B., 2005b. Experimental measurements and modeling of sorption competition on montmorillonite. Geochim. Cosmochim. Acta 69, 4187–4197.
Bradbury, M.H., Baeyens, B., 2009a. Sorption modelling on illite. Part II: Actinide sorption and linear free energy relationships. Geochim. Cosmochim. Acta 73, 1004–1013.
Bradbury, M.H., Baeyens, B., 2009b. Sorption modelling on illite Part I: Titration measurements and the sorption of Ni, Co, Eu and Sn. Geochim. Cosmochim. Acta 73, 990–1003.
Bradbury, M.H., Baeyens, B., 2009c. Experimental and modelling studies on the pH buffering of MX-80 bentonite porewater. Appl. Geochem. 24, 419–425.
Bradbury, M.H., Baeyens, B., 2011. Predictive sorption modelling of Ni(II), Co(II), Eu (IIII), Th(IV) and U(VI) on MX-80 bentonite and Opalinus Clay: a "bottom-up" approach. Appl. Clay Sci. 52, 27–33.
Bradbury, M.H., Baeyens, B., Geckeis, H., Rabung, T., 2005. Sorption of Eu(III)/Cm(III) on Ca-montmorillonite and Na-illite. Part 2: Surface complexation modelling. Geochim. Cosmochim. Acta 69, 5403–5412.
Businelli, M., Casciari, F., Businelli, D., Gigliotti, G., 2003. Mechanisms of Pb (II) sorption and desorption at some clays and goethite-water interfaces. Agron. EDP Sci. 23, 219–225.
Centofanti, T., Siebecker, M.G., Chaney, R.L., Davis, A.P., Sparks, D.L., 2012. Hyperaccumulation of nickel by Alyssum corsicum is related to solubility of Ni mineral species. Plant Soil 359, 71–83.
Charlet, L., Schindler, P.W., Spadini, L., Furrer, G., Zysset, M., 1993. Cation adsorption on oxides and clays: the aluminum case. Aquat. Sci. 55, 1015–1621.
Chen, L., Dong, Y., 2013. Sorption of 63Ni(II) to montmorillonite as a function of pH, ionic strength, foreign ions and humic substances. J. Radioanal. Nucl. Chem. 295, 2117–2123.

Chen, C., Hayes, F., 1999. X-Ray absorption spectroscopy investigation of aqueous Co(II) and Sr(II) sorption at clay-water interfaces. Geochim. Cosmochim. Acta 63, 3205–3215.
Chen, Z., Montavon, G., Guo, Z., Wang, X., Razafindratsima, S., Robinet, J.C., Landesman, C., 2014a. Approaches to surface complexation modeling of Ni (II) on Callovo-Oxfordian clayrock. Appl. Clay Sci. 101, 369–380.
Chen, Z., Montavon, G., Ribet, S., Guo, Z., Robinet, J.C., David, K.K., Tournassat, C., Grambow, B., Landesman, C., 2014b. Key factors to understand in-situ behavior of Cs in Callovo-Oxfordian clay-rock (France). Chem. Geol. 387, 47–58.
Chen, Z., Chen, L., Lu, S., 2016. Effect of solution chemistry on the interaction of radionuclide 63Ni(II) onto montmorillonite. J. Radioanal. Nucl. Chem. 308, 505–516.
Churakov, S.V., Dähn, R., 2012. Zinc adsorption on clays inferred from atomistic simulations and EXAFS spectroscopy. Environ. Sci. Technol. 46, 5713–5719.
Claret, F., Lerouge, C., Laurioux, T., Bizi, M., Conte, T., Ghestem, J.P., Wille, G., Sato, T., Gaucher, E.C., Giffaut, E., Tournassat, C., 2010. Natural iodine in a clay formation: Implications for iodine fate in geological disposals. Geochim. Cosmochim. Acta 74, 16–29.
Dähn, R., Scheidegger, A.M., Manceau, A., Schlegel, M., Baeyens, B., Bradbury, M.H., M. schl. Morales., 2002. Neoformation of Ni phyllosilicate upon Ni uptake on montmorillonite: a kinetics study by powder and polarized extended X-ray absorption fine structure spectroscopy. Geochim. Cosmochim. Acta 66, 2335–2347.
Dähn, R., Scheidegger, A.M., Manceau, A., Schlegel, M., Baeyens, B., Bradbury, M.H., Chateigner, D.L., 2003. Structural evidence for the sorption of Ni(II) atoms on the edges of montmorillonite clay minerals: a polarized X-ray absorption fine structure study. Geochim. Cosmochim. Acta 37, 1–15.
Dähn, R., Baeyens, B., Bradbury, M.H., 2011. Investigation of the different binding edge sites for Zn on montmorillonite using P-EXAFS - the strong/weak site concept in the 2SPNE SC/CE sorption model. Geochim. Cosmochim. Acta 75, 5154–5168.
De Windt, L., Pellegrini, D., Van der Lee, J., 2004. Coupled modeling of cement/claystone interactions and radionuclide migration. J. Contam. Hydrol. 68, 165–182.
Du, Q., Sun, Z., Forsling, W., Tang, H., 1997. Adsorption of copper at aqueous illite surfaces. J. Colloid Interface Sci. 187, 232–242.
Echeverría, J.C., Zarranz, I., Estella, J., Garrido, J.J., 2005. Simultaneous effect of pH, temperature, ionic strength, and initial concentration on the retention of lead on illite. Appl. Clay Sci. 30, 103–115.
Elzinga, E.J., Sparks, D.L., 2001. Reaction condition effects on nickel sorption mechanisms in illite-water suspensions. Soil Sci. Soc. Am. J. 65, 94–101.
Fan, Q., Li, P., Pan, D., Chen, C., 2019. Chapter 1 - Radionuclides sorption on typical clay minerals: Modeling and spectroscopies. In: Emerging Natural and Tailored Nanomaterials for Radioactive Waste Treatment and Environmental Remediation. Elsevier, pp. 1–38.
Fletcher, P., Sposito, G., 1989. The chemical modeling of clay/electrolyte interactions for montmorillonite. Clay Miner. 24, 375–391.
Ford, R.G., Scheinost, A.C., Scheckel, K.G., Sparks, D.L., 1999. The link between clay mineral weathering and the stabilization of Ni surface precipitates. Environ. Sci. Technol. 33, 3140–3144.
Fralova, L., Lefèvre, G., Madé, B., Marsac, R., Thory, E., Dagnelie, R.V.H., 2021. Effect of organic compounds on the retention of radionuclides in clay rocks: Mechanisms and specificities of Eu(III), Th(IV), and U(VI). Appl. Geochem. 127, 104859.
Gailhanou, H., Lerouge, C., Debure, M., Gaboreau, S., Gaucher, E.C., Grangeon, S., Grenèche, J.-M., Kars, M., Madé, B., Marty, N.C.M., Warmont, F., Tournassat, C., 2017. Effects of a thermal perturbation on mineralogy and pore water composition in a clay-rock: an experimental and modeling study. Geochim. Cosmochim. Acta 197, 193–214.
Gao, P., Liu, X., Guo, Z., Tournassat, C., 2023. Acid-base properties of cis-vacant montmorillonite edge surfaces: a combined first-principles molecular dynamics and surface complexation modeling approach. Environ. Sci. Technol. 57, 1342–1352.
Garcia-Miragaya, J., Page, A.L., 1976. Influence of ionic-strength and inorganic complex-formation on sorption of trace amounts of Cd by montmorillonite. Soil Sci. Soc. Am. J. 40 (658–633).
Ghayaza, M., Le Forestier, L., Muller, F., Tournassat, C., Beny, J.M., 2011. Pb(II) and Zn (II) adsorption onto Na- and Ca-montmorillonites in acetic acid/acetate medium: Experimental approach and geochemical modeling. J. Colloid Interface Sci. 361, 238–246.
Giffaut, E., Grivé, M., Blanc, P., Vieillard, P., Colàs, E., Gailhanou, H., Gaboreau, S., Marty, N., Madé, B., Duro, L., 2014. Andra thermodynamic database for performance assessment: ThermoChimie. Appl. Geochem. 49, 225–236.
Gräfe, M., Singh, B., Balasubramanian, M., 2007. Surface speciation of Cd(II) and Pb(II) on kaolinite by XAFS spectroscopy. J. Colloid Interface Sci. 315, 21–32.
Grambow, B., 2016. Geological disposal of radioactive waste in clay. Elements 12, 239–245.
Grambow, B., Fattahi, M., Montavon, G., Moisan, C., Giffaut, E., 2006. Sorption of Cs, Ni, Pb, Eu(III), Am(III), Cm, Ac(III), Tc(IV), Th, Zr, and U(VI) on MX80 bentonite: an experimental approach to assess model uncertainty. Radiochim. Acta 94, 627–636.
Grangeon, S., Vinsot, A., Tournassat, C., Lerouge, C., Giffaut, E., Heck, S., Groschopf, N., Denecke, M.A., Wechner, S., Schäfer, T., 2015. The influence of natural trace element distribution on the mobility of radionuclides. The exemple of nickel in a clay-rock. Appl. Geochem. 52, 155–173.
Green-Pedersen, H., Pind, N., 2000. Preparation, characterization, and sorption properties for Ni(II) of iron oxyhydroxide-montmorillonite. Colloids and Surf. A-Physicochem. Engineer. Aspects 168, 133–145.
Gu, X.Y., Evans, L.J., Barabash, S.J., 2010. Modeling the adsorption of Cd (II), Cu (II), Ni (II), Pb (II) and Zn (II) onto montmorillonite. Geochim. Cosmochim. Acta 74, 5718–5728.
Hautevelle, Y., Michels, R., Malartre, F., Elie, M., Trouiller, A., 2007. Tracing of variabilities within a geological barrier by molecular organic geochemistry. Case of the Callovo-Oxfordian sedimentary series in the East of the Paris Basin (France). Appl. Geochem. 22, 736–759.
Hu, T., Tan, L., 2012. Sorption/desorption of radionickel on/from Na-montmorillonite: kinetic and thermodynamic studies. J. Radioanal. Nucl. Chem. 292, 103–112.
Hu, W., Lu, S., Song, W., Chen, T., Hayat, T., Alsaedi, N.S., Chen, C., Liu, H., 2018. Competitive adsorption of U(VI) and Co(II) on montmorillonite: a batch and spectroscopic approach. Appl. Clay Sci. 157, 121–129.
Hyun, S.P., Hayes, K.F., 2004. Copper (II) sorption mechanism on kaolinite: an EPR and EXAFS study. J. Mineral. Soc. Korea 17, 1–9.
Ikhsan, J., Wells, J.D., Johnson, B.B., Angove, M.J., 2005. Surface complexation modeling of the sorption of Zn(II) by montmorillonite. Colloids and Surf. A-Physicochem. Engineer. Aspects 252, 33–41.
Kraepiel, A.M.L., Keller, K., Morel, F.M.M., 1999. A model for metal adsorption on montmorillonite. J. Colloid Interface Sci. 210, 43–54.
Kulik, D.A., 2009. Thermodynamic concepts in modeling sorption at the mineral-water interface. Rev. Mineral. Geochem. 70, 125–180.
Lázár, K., Máthé, Z., 2012. Claystone as a potential host rock for nuclear waste storage. Clay minerals in nature–their characterization, modification and application. Intech 56–80.
Lee, S., Anderson, P.R., Bunker, G.B., Karanfil, C., 2004. EXAFS study of Zn sorption mechanisms on montmorillonite. Environ. Sci. Technol. 38, 5426–5432.
Legates, D.R., McCabe, G.J., 1999. Evaluating the use of"goodness-of-fit" measures in hydrologic and hydroclimaticmodel validation. Water Resour. Res. 35, 233–241.
Li, J., Hu, J., Sheng, G., Zhao, G., Huang, Q., 2009. Effect of pH, ionic strength, foreign ions and temperature on the adsorption of Cu(II) from aqueous solution to GMZ bentonite. Colloids Surf. A Physicochem. Eng. Asp. 349, 195–201.
Liu, X., Tournassat, C., Grangeon, S., Kalinichev, A.G., Takahashi, Y., Marques Fernandes, M., 2022. Molecular-level understanding of metal ion retention in clay-rich materials. Nat. Rev. Earth Environ. 3, 461–476.
Lothenbach, B., Furrer, G., Schulin, R., 1997. Immobilization of heavy metals by polynuclear aluminium and montmorillonite compounds. Environ. Sci. Technol. 31, 1452–1462.
Malekifarsani, A., Skachek, M.A., 2009. Effect of precipitation, sorption and stable of isotope on maximum release rates of radionuclides from engineered barrier system (EBS) in deep repository. J. Environ. Radioact. 100, 807–814.
Marani, D., Macchi, G., Pagano, M., 1995. Lead precipitation in the presence of sulphate and carbonate: Testing of thermodynamic predictions. Water Res. 29, 1085–1092.
Marcussen, H., Holm, P.E., Strobel, B.W., Hansen, H.C.B., 2009. Nickel sorption to goethite and montmorillonite in presence of citrate. Environ. Sci. Technol. 43, 1122–1127.
Marques Fernandes, M., Baeyens, B., 2019. Cation exchange and surface complexation of lead on montmorillonite and illite including competitive adsorption effects. Appl. Geochem. 100, 190–202.
Marques Fernandes, M., Ver, N., Baeyens, B., 2015. Predicting the uptake of Cs, Co, Ni, Eu, Th and U on argillaceous rocks using sorption models for illite. Appl. Geochem. 59, 189–199.
Marques Fernandes, M., Scheinost, A., Baeyens, B., 2016. Sorption of trivalent lanthanides and actinides onto montmorillonite: Macroscopic, thermodynamic and structural evidence for ternary hydroxo and carbonato surface complexes on multiple sorption sites. Water Res. 99, 74–82.
Montavon, G., Sabatié-Gogova, A., Ribet, S., Bailly, C., Bessaguet, N., Durce, D., Giffaut, E., Landesman, C., Grambow, B., 2014. Retention of iodide by the Callovo-Oxfordian formation: an experimental study. Appl. Clay Sci. 87, 142–149.
Montavon, G., Lerouge, C., David, K., Ribet, S., Hassan-Loni, Y., Leferrec, M., Bailly, C., Robinet, J.-C., Grambow, B., 2020. Nickel retention on callovo-oxfordian clay: applicability of existing adsorption models for dilute systems to real compact rock. Environ. Sci. Technol. 54 (19), 12226–12234.
Morel, F.M.M., 1997. Discussion on: "a mechanistic description of Ni and Zn sorption on Na-montmorillonite. Part I: Titration and sorption measurements. Part II: modelling" by Bart Baeyens and Michael H. Bradbury. J. Contam. Hydrol. 28, 7–10.
Morel, F.M.M., Kraepiel, A.M.L., 1997. Further comment: Coulombic effects on the adsorption of trace cations on clays. J. Contam. Hydrol. 28, 17–20.
Moriasi, D.N., Arnold, J.G., Liew, M.W.V., Bingner, R.L., Harmel, R.D., Veith, T.L., 2007. Model evaluation guidelines for systematic quantification of accuracy in watershed simulations. Trans. ASABE 50, 885–900.
Morton, J.D., Semrau, J.D., Hayes, K.F., 2001. An X-ray absorption spectroscopy study of the structure and reversibility of copper adsorbed to montmorillonite clay. Geochim. Cosmochim. Acta 65, 2709–2722.
Nash, K.E., Sutcliffe, J.V., 1970. River flow forecasting through conceptual models: 1- a discussion of principles. J. Hydrol. 10, 282–290.
O'Day, P.A., Brown, G.E., Parks, G.A., 1994. X-Ray absorption spectroscopy of cobalt(II) multinuclear surface complexes and surface precipitates on kaolinite. J. Colloid Interface Sci. 165, 269–289.
Orucoglu, E., Tournassat, C., Robinet, J.-C., Madé, B., Lundy, M., 2018. From experimental variability to the sorption related retention parameters necessary for performance assessment models for nuclear waste disposal systems: the example of Pb adsorption on clay minerals. Appl. Clay Sci. 163, 20–32.
Orucoglu, E., Grangeon, S., Gloter, A., Robinet, J.-C., Madé, B., Tournassat, C., 2022. Competitive adsorption processes at clay mineral surfaces: a coupled experimental and modeling approach. ACS Earth Space Chem. 6, 144–159.
Papelis, C., Hayes, K.F., 1996. Distinguishing between interlayer and external sorption sites of clay minerals using X-ray absorption spectroscopy. Colloids and Surf. A-Physicochem. Engineer. Aspects 107, 89–96.

Papelis, C., Brown, G.E., Parks, G.A., Leckie, J.O., 1995. X-ray absorption spectroscopic studies of cadmium and selenite adsorption on aluminum oxides. Langmuir 11, 2041–2048.
Parkhurst, D.L., Appelo, C.A.J., 2013. Description of Input and Examples for PHREEQC Version 3–a Computer Program for Speciation, Batch-Reaction, One-Dimensional Transport, and Inverse Geochemical Calculations.
Pfingsten, W., Bradbury, M., Baeyens, B., 2011. The influence of Fe(II) competition on the sorption and migration of Ni(II) in MX-80 bentonite. Appl. Geochem. 26, 1414–1422.
R_Core_Team, 2020. R: A Language and Environment for Statistical ComputingVersion 4.0.3. R Foundation for Statistical Computing, Vienna, Austria.
Scheidegger, A.M., Fendorf, M., Sparks, D.L., 1996. Mechanisms of nickel sorption on pyrophyllite: macroscopic and microscopic approaches. Soil Sci. Soc. Am. J. 60, 1763–1772.
Scheidegger, A.M., Strawn, D.G., Lamble, G.M., Sparks, D.L., 1998. The kinetics of mixed Ni-Al hydroxide formation on clay and aluminum oxide minerals: a time-resolved XAFS study. Geochim. Cosmochim. Acta 62, 2233–2245.
Scheinost, A.C., Sparks, D.L., 2000. Formation of layered single- and double-metal hydroxide precipitates at the mineral/water interface: a multiple-scattering XAFS analysis. J. Colloid Interface Sci. 223, 167–178.
Schlegel, M.L., Manceau, A., Charlet, L., Chateigner, D.L., Hazemann, J.L., 2001a. Sorption of metal ions on clay minerals. III. Nucleation and epitaxial growth of Zn phyllosilicate on the edges of hectorite. Geochim. Cosmochim. Acta 65, 4155–4470.
Schlegel, M., Manceau, A., Charlet, L., Hazemann, J.L., 2001b. Adsorption mechanisms of Zn on hectorite as a function of time, pH, and ionic strength. Am. J. Sci. 301, 798–830.
Shao, D.D., Xu, D., Wang, S.W., Fang, Q.H., Wu, W.S., Dong, Y.H., Wang, X.K., 2009. Modeling of radionickel sorption on MX-80 bentonite as a function of pH and ionic strength. Sci. China Ser. B-Chem. 52, 362–371.
Sochala, P., Chiaberge, C., Claret, F., Tournassat, C., 2022. Uncertainty propagation in pore water chemical composition calculation using surrogate models. Sci. Rep. 12, 15077.
Sochala, P., Chiaberge, C., Claret, F., Tournassat, C., 2024. Dimension reduction for uncertainty propagation and global sensitivity analyses of a cesium adsorption model. J. Comput. Sci. 75, 102197.
Soltermann, D., Fernandes, M.M., Baeyens, B., Daehn, R., Miehe-Brendle, J., Wehrli, B., Bradbury, M.H., 2013. Fe(II) sorption on a synthetic montmorillonite. A combined macroscopic and spectroscopic study. Environ. Sci. Technol. 47, 6978–6986.
Strawn, D.G., Sparks, D.L., 1999. The use of XAFS to distinguish between inner- and outer-sphere lead adsorption complexes on montmorillonite. J. Colloid Interface Sci. 216, 257–269.
Tertre, E., Berger, G., Castet, S., Loubet, M., Giffaut, E., 2005. Experimental sorption of Ni^{2+}, Cs^{+} and Ln^{3+} onto a montmorillonite up to 150ęgreC. Geochim. Cosmochim. Acta 69, 4937–4948.
Tournassat, C., Ferrage, E., Poinsignon, C., Charlet, L., 2004. The titration of clay minerals II. Structure-based model and implications for clay reactivity. J. Colloid Interface Sci. 273, 234–246.
Tournassat, C., Grangeon, S., Leroy, P., Giffaut, E., 2013. Modeling specific pH dependent sorption of divalent metals on montmorillonite surfaces. A review of pitfalls, recent achievements and current challenges. Am. J. Sci. 313, 395–451.
Tournassat, C., Vinsot, A., Gaucher, E.C., Altmann, S., 2015. Chapter 3 - Chemical conditions in clay-rocks. Pages 71–100. In: Tournassat, C., Steefel, C.I., Bourg, I.C., Bergaya, F. (Eds.), Natural and Engineered Clay Barriers. Elsevier.
Tournassat, C., Davis, J.A., Chiaberge, C., Grangeon, S., Bourg, I.C., 2016. Modeling the acid–base properties of montmorillonite edge surfaces. Environ. Sci. Technol. 50, 13436–13445.
Tournassat, C., Tinnacher, R.M., Grangeon, S., Davis, J.A., 2018. Modeling uranium(VI) adsorption onto montmorillonite under varying carbonate concentrations: a surface complexation model accounting for the spillover effect on surface potential. Geochim. Cosmochim. Acta 220, 291–308.
Turner, D.R., Pabalan, R.T., Bertetti, F.P., 1998. Neptunium(V) sorption on montmorillonite: an experimental and surface complexation modeling study. Clay Clay Miner. 46, 256–269.
Vasconcelos, I.F., Haack, E.A., Maurice, P.A., Bunker, B.A., 2008. EXAFS analysis of cadmium(II) adsorption to kaolinite. Chem. Geol. 249, 237–249.
Wang, S., Dong, Y., He, M., Chen, L., Yu, X., 2009. Characterization of GMZ bentonite and its application in the adsorption of Pb(II) from aqueous solutions. Appl. Clay Sci. 43, 164–171.
Wen, T., Chen, Y., Cai, L., 2011. Impact of environmental conditions on the sorption behavior of radiocobalt onto montmorillonite. J. Radioanal. Nucl. Chem. 290.
Woodward, G.L., Peacock, C.L., Otero-Fariña, A., Thompson, O.R., Brown, A.P., Burke, I. T., 2018. A universal uptake mechanism for cobalt(II) on soil constituents: Ferrihydrite, kaolinite, humic acid, and organo-mineral composites. Geochim. Cosmochim. Acta 238, 270–291.
Wu, X.L., Zhao, D., Yang, S.T., 2011. Impact of solution chemistry conditions on the sorption behavior of Cu(II) on Lin'an montmorillonite. Desalination 269, 84–91.
Yang, S., Zhao, D., Zhang, H., Lu, S., Chen, X.L. Yu, 2010. Impact of environmental conditions on the sorption behavior of Pb (II) in Na-bentonite suspensions. J. Hazard. Mater. 183, 632–640.
Yang, S., Ren, X., Zhao, G., Shi, W., Montavon, G., Grambow, B., Wang, X., 2015. Competitive sorption and selective sequence of Cu(II) and Ni(II) on montmorillonite: batch, modeling, EPR and XAS studies. Geochim. Cosmochim. Acta 166, 129–145.
Yu, S., Wang, X., Chen, Z., Tan, X., Wang, H., Hu, J., Alsaedi, A., Alharbi, N.S., Guo, W., Wang, X., 2016. Interaction mechanism of radionickel on Na-montmorillonite: Influences of pH, electrolyte cations, humic acid and temperature. Chem. Eng. J. 302, 77–85.
Zachara, J.M., Smith, S.C., McKinley, J.P., Resch, C.T., 1993. Cadmium sorption on specimen and soil smectites in sodium and calcium electrolytes. Soil Sci. Soc. Am. J. 57, 1491–1501.
Zhang, C., Liu, X., Tinnacher, R.M., Tournassat, C., 2018. Mechanistic understanding of uranyl ion complexation on montmorillonite edges: a combined first-principles molecular dynamics-surface complexation modeling approach. Environ. Sci. Technol. 52, 8501–8509.